

Dynamic and bending analysis of carbon nanotube-reinforced composite plates with elastic foundation

Boumediene Bakhadda^{1,2}, Mohamed Bachir Bouiadjra^{1,8}, Fouad Bourada³,
Abdelmoumen Anis Bousahla^{4,5}, Abdelouahed Tounsi^{*2,6,8} and S.R. Mahmoud⁷

¹Laboratoire des Structures et Matériaux Avancés dans le Génie Civil et Travaux Publics, Université de Sidi Bel Abbès,
Faculté de Technologie, Département de génie civil, Algeria

²Material and Hydrology Laboratory, University of Sidi Bel Abbès, Faculty of Technology, Civil Engineering Department, Algeria

³Département de Génie Civil, Institut de Technologie, Centre Universitaire de Ain Témouchent, Algeria

⁴Laboratoire de Modélisation et Simulation Multi-échelle, Département de Physique, Faculté des Sciences Exactes,
Département de Physique, Université de Sidi Bel Abbès, Algeria

⁵Centre Universitaire Ahmed Zabana de Relizane, Algeria

⁶Department of Civil and Environmental Engineering, King Fahd University of Petroleum & Minerals,
31261 Dhahran, Eastern Province, Saudi Arabia

⁷Department of Mathematics, Faculty of Science, King Abdulaziz University, Jeddah, Saudi Arabia

⁸Algerian National Thematic Agency of Research in Science and Technology (ATRST), Algeria

(Received November 19, 2017, Revised January 24, 2018, Accepted February 2, 2018)

Abstract. This work examines vibration and bending response of carbon nanotube-reinforced composite plates resting on the Pasternak elastic foundation. Four types of distributions of uni-axially aligned single-walled carbon nanotubes are considered to reinforce the plates. Analytical solutions determined from mathematical formulation based on hyperbolic shear deformation plate theory are presented in this study. An accuracy of the proposed theory is validated numerically by comparing the obtained results with some available ones in the literature. Various considerable parameters of carbon nanotube volume fraction, spring constant factors, plate thickness and aspect ratios, etc. are considered in the present investigation. According to the numerical examples, it is revealed that the vertical displacement of the plates is found to diminish as the increase of foundation parameters; while, the natural frequency increase as the increment of the parameters for every type of plate.

Keywords: bending; vibration; CNTRC plate; plate theory

1. Introduction

Carbon nanotubes (CNTs) have excellent mechanical characteristics and because of their outstanding properties such as, superior mechanical, electrical, and thermal nanotubes have attracted growing interest and are considered to be the most promising materials for applications in nanoengineering (Lau and Hui 2002, Lau *et al.* 2004, Esawi and Farag 2007). So many applications for CNTs have been developed by researchers: conductive polymers; energy conversion devices and energy storage; sensors; field emission displays; replacing silicon in microcircuits; multilevel chips; probes for SPM (scanning probe microscopy) (Esawi and Farag 2007). To provide high performance structural and multifunctional composites for different potential applications, CNTs which have high elastic modulus, tensile strength and low density can be employed as reinforcing constituents instead of conventional fibers. The earliest investigation on carbon nanotube-reinforced composites (CNTRCs) fabricated from polymer reinforced by aligned CNT arrays had been

presented in the work of Ajayan *et al.* (1994), and since then many researchers have paid their attention on studying material properties of the CNTRCs (Odegard *et al.* 2003, Griebel and Hamaekers 2004, Mokashi *et al.* 2007). Moreover, to introduce thermal influence on material properties of nanocomposites provided from polymer and CNTs, it was developed by Fidelus *et al.* (2005). In terms of macro scale, Hu *et al.* (2005) presented the formulation for determining the elastic properties of CNTRCs and the elastic deformation of a representative volume element under different loading conditions was examined in the work. By employing molecular dynamics (MD), the elastic characteristics of CNTRCs can be predicted (Han and Elliott 2007). Zhu *et al.* (2007) discussed the stress-strain curves of CNT-reinforced Epon 862 composites which demonstrate that the mechanical, electrical and thermal properties of the composite materials can be improved considerably with the incorporation of small amounts of CNTs to polymer matrix. In order to understand more about how to enhance dispersion and alignment of CNTs in a polymer matrix, Xie *et al.* (2005) presented the existing methods employed for this purpose.

Recently, many plate theories are developed in literature such as (Yazid *et al.* 2018, Meksi *et al.* 2018, Youcef *et al.* 2018, Attia *et al.* 2018, Zine *et al.* 2018, Chikh *et al.* 2017, Kolahchi *et al.* 2017a,b, Abdelaziz *et al.* 2017,

*Corresponding author, Professor
E-mail: tou_abdel@yahoo.com

Hajmohammad *et al.* 2017, Sekkal *et al.* 2017a, Fahsi *et al.* 2017, Hachemi *et al.* 2017, Aldousari 2017, Shokravi (2017a), Kolahchi 2017, Khetir *et al.* 2017, Bellifa *et al.* 2017a, b, El-Haina *et al.* 2017, Besseghier *et al.* 2017, Zidi *et al.* 2017, Klouche *et al.* 2017, Menasria *et al.* 2017, Mouffoki *et al.* 2017, Bousahla *et al.* 2016, Houari *et al.* 2016, Kolahchi *et al.* 2016a, Ebrahimi and Habibi 2016, Ghorbanpour Arani *et al.* 2016, Barati and Shahverdi 2016, Beldjelili *et al.* 2016, Bounouara *et al.* 2016, Boukhari *et al.* 2016, Boudierba *et al.* 2016, Ahouel *et al.* 2016, Bellifa *et al.* 2016, Belkorissat *et al.* 2015, Mahi *et al.* 2015, Ait Yahia *et al.* 2015, Attia *et al.* 2015, Taibi *et al.* 2015, Zemri *et al.* 2015, Zidi *et al.* 2014, Hebali *et al.* 2014, Ahmed 2014, Boudierba *et al.* 2013, Tounsi *et al.* 2013). In cases of 2D analyses of CNTRC structures, bending and dynamic behaviors of CNTRC plates, were solved by employing finite element method with the first order shear deformation theory (FSDT) (Zhu *et al.* 2012). Lei *et al.* (2013) analyzed stability strength of three different kinds of CNTRC plates having symmetrical repartition of CNTs, by employing the element-free kp-Ritz method. Shen and Zhang (2010) provided the solutions for critical stability temperature and thermal post-buckling response of two layer CNTRC plates with symmetrically distributed CNTs. The nonlinear dynamic response of CNTRC plates subjected to temperature was discussed by Wang and Shen (2011). Kolahchi *et al.* (2017b) studied the wave propagation of embedded viscoelastic FG-CNT-reinforced sandwich plates integrated with sensor and actuator based on refined zigzag theory. Zamanian *et al.* (2017) examined agglomeration effects on the buckling behaviour of embedded concrete columns reinforced with SiO₂ nano-particles. Kolahchi *et al.* (2017c) investigated wave propagation of embedded viscoelastic FG-CNT-reinforced sandwich plates integrated with sensor and actuator based on refined zigzag theory. Bilouei *et al.* (2016) investigated the buckling of concrete columns retrofitted with Nano-Fiber Reinforced Polymer (NFRP). Kolahchi *et al.* (2016b) discussed the vibration stability response of temperature-dependent functionally graded CNT-reinforced visco-plates resting on orthotropic elastomeric medium. Madani *et al.* (2016) presented differential cubature method for vibration analysis of embedded FG-CNT-reinforced piezoelectric cylindrical shells subjected to uniform and non-uniform temperature distributions. Kolahchi and Bidgoli (2016) presented a size-dependent sinusoidal beam model for dynamic instability of single-walled carbon nanotubes. Zarei *et al.* (2017) examined seismic response of underwater fluid-conveying concrete pipes reinforced with SiO₂ nanoparticles and fiber reinforced polymer (FRP) layer. Shokravi (2017b) presented vibration analysis of silica nanoparticles-reinforced concrete beams considering agglomeration effects. Arani and Kolahchi (2016) analyzed buckling response of embedded concrete columns armed with carbon nanotubes. Shokravi (2017c) presented buckling analysis of embedded laminated plates with agglomerated CNT-reinforced composite layers using FSDT and DQM. Using Reddy plate theory, Shokravi (2017d) studied buckling of sandwich plates with FG-CNT-reinforced layers resting on orthotropic elastic medium. Mehar and Panda (2017a)

presented a thermoelastic analysis of FG-CNT reinforced shear deformable composite plate under various loading. In the same way, Mehar and Panda (2017b) studied the Thermoelastic nonlinear vibration behavior of CNT reinforced functionally graded sandwich structure. Using Bolotin method, Kolahchi and Cheraghbak (2017) studied agglomeration effects on the dynamic buckling of viscoelastic microplates reinforced with SWCNTs.

In this work, CNTRC plates supported by the Pasternak elastic foundation are examined. Generalized shear deformation plate model is utilized to obtain the equations of motions. Various accurate solutions of vertical displacements, stresses and natural frequencies of such plates are illustrated and discussed in relation to several important aspects such as plate thickness and aspect ratios, spring constant factors, volume fraction of CNTs and plate types.

2. CNTRC plates

In this work, a CNTRC plate has dimensions ($a \times b \times h$) such as " a " is length, " b " width and " h " thickness. The plate is resting on the elastic foundation, including Winkler springs and shear layer as illustrated in Fig. 1. types of the carbon nanotube distributions across the thickness for reinforced the CNTRC plate are assumed (UD-plate, O-plate, X-plate and V-plate). In Fig. 1 it should be noted that the symmetrical distribution of SWCNTs is for O-plate and X-plate, on the other hand the uniform distribution of SWCNTs is for UD-plate, and V-plate distribution has a variable distribution along the thickness direction. Since, the plate is assumed to consist of SWCNT mixture with a gradual distribution through the thickness and isotropic matrix. Using a rule of mixture we determine the effective material properties of the CNTRC. The effective Young's modulus and shear modulus can be expressed as (Shen 2009)

$$E_{11} = \eta_1 V_{cnt} E_{11}^{cnt} + V_p E^p \quad (1a)$$

$$\frac{\eta_2}{E_{22}} = \frac{V_{cnt}}{E_{22}^{cnt}} + \frac{V_p}{E^p} \quad (1b)$$

$$\frac{\eta_3}{G_{12}} = \frac{V_{cnt}}{G_{12}^{cnt}} + \frac{V_p}{G^p} \quad (1c)$$

Where (E_{11}, E_{22}) , $(E_{11}^{cnt}, E_{22}^{cnt})$, and (E^p) are the Young's modulus of the composite, the carbon nanotube and the polymer, respectively. (G_{12}) is the shear modulus of composite and $\eta_j (j=1,2,3)$ is the CNT efficiency parameter. V_{cnt} and V_p indicate the volume fraction of the CNTs and the polymer, respectively. With $(V_{cnt} + V_p = 1)$.

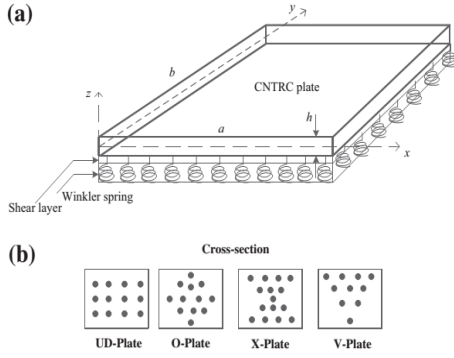


Fig. 2 Geometry of a CNTRC plate resting on the Pasternak elastic foundation (a) and cross-sections with different patterns of carbon nanotube reinforcement (b)

The poisson's ratio and the mass density can be written as follows

$$\nu_{12} = V_{cnt} \nu_{12}^{cnt} + V_p \nu^p; \rho = V_{cnt} \rho^{cnt} + V_p \rho^p \quad (2)$$

The mathematical models of the four patterns of reinforcement over the plate thickness (UD, O, X and V) describing the materials distribution can be expressed as Eqs. (3(a)-3(d))

$$UD - plate : V_{cnt} = V_{cnt}^* \quad (3a)$$

$$O - plate : V_{cnt} = 2(1 - 2\frac{|z|}{h})V_{cnt}^* \quad (3b)$$

$$X - plate : V_{cnt} = 4\frac{|z|}{h}V_{cnt}^* \quad (3c)$$

$$V - plate : V_{cnt} = (1 + \frac{2z}{h})V_{cnt}^* \quad (3d)$$

With

$$V_{cnt}^* = \frac{W_{cnt}}{W_{cnt} + (\rho^{cnt} / \rho^m)(1 - W_{cnt})} \quad (4)$$

Where V_{cnt}^* represent the mass fraction of CNTs.

The carbon nanotube efficiency parameters (η_j) used in this works are $\eta_1 = 0.149$ and $\eta_2 = \eta_3 = 0.934$ for the case of $V_{cnt}^* = 0.11$; $\eta_1 = 0.150$ and $\eta_2 = \eta_3 = 0.941$ for the case of $V_{cnt}^* = 0.14$; $\eta_1 = 0.149$ and $\eta_2 = \eta_3 = 1.381$ for the case of $V_{cnt}^* = 0.17$ (Zhu *et al.* 2012, Wattanasakulpong and Chaikittiratanana 2015).

3. Displacement field and strains of CNTRC plates

Considering a thick CNTRC plate, the hyperbolic shear deformation plate theory was employed to account for the

displacement field (u, v, w) within a plate domain. The displacement field can be written as

$$u(x, y, z, t) = u_0(x, y, t) - zw_{0,x} - \psi(z)\varphi_x \quad (5a)$$

$$v(x, y, z, t) = v_0(x, y, t) - zw_{0,y} - \psi(z)\varphi_y \quad (5b)$$

$$w(x, y, z, t) = w_0(x, y, t) \quad (5c)$$

With

$$\psi(z) = \frac{1}{2}h \tanh(\frac{2z}{h}) - \frac{4}{3} \frac{z^3}{h^2 \cosh(1)^2} \quad (6)$$

where $\psi(z)$ is the warping function. In this study, the shape function in Eq. (6) is expressed by a hyperbolic function and assures an accurate distribution of shear deformation through the CNTRC plate thickness and allows to transverse shear stresses vary as parabolic across the thickness as satisfying shear stress free surface conditions without using shear correction factors. Indeed, it should be mentioned that contrary to the first shear deformation theory (FSDT), the proposed theory does not require shear correction factors.

The strain components associated with the displacement field based on HSDT in Eq. (5) can be obtained as

$$\varepsilon_{xx} = \frac{\partial u_0}{\partial x} - z \frac{\partial^2 w_0}{\partial x^2} + \psi(z) \frac{\partial \varphi_x}{\partial x} \quad (7a)$$

$$\varepsilon_{yy} = \frac{\partial v_0}{\partial y} - z \frac{\partial^2 w_0}{\partial y^2} + \psi(z) \frac{\partial \varphi_y}{\partial y} \quad (7b)$$

$$\gamma_{xy} = \frac{\partial u_0}{\partial y} + \frac{\partial v_0}{\partial x} - 2z \frac{\partial^2 w_0}{\partial x \partial y} + \psi(z) (\frac{\partial \varphi_x}{\partial y} + \frac{\partial \varphi_y}{\partial x}) \quad (7c)$$

$$\gamma_{xz} = \frac{\partial \psi(z)}{\partial z} \varphi_x; \gamma_{yz} = \frac{\partial \psi(z)}{\partial z} \varphi_y \quad (7d)$$

The expression of the constitutive relations can be written in the form

$$\begin{Bmatrix} \sigma_{xx} \\ \sigma_{yy} \\ \sigma_{xy} \end{Bmatrix} = \begin{bmatrix} Q_{11} & Q_{12} & 0 \\ Q_{12} & Q_{22} & 0 \\ 0 & 0 & Q_{66} \end{bmatrix} \begin{Bmatrix} \varepsilon_{xx} \\ \varepsilon_{yy} \\ \varepsilon_{xy} \end{Bmatrix}; \begin{Bmatrix} \sigma_{yz} \\ \sigma_{xz} \end{Bmatrix} = \begin{bmatrix} Q_{44} & 0 \\ 0 & Q_{55} \end{bmatrix} \begin{Bmatrix} \gamma_{yz} \\ \gamma_{xz} \end{Bmatrix} \quad (8)$$

Where, the stiffness coefficients can be expressed as

$$Q_{11} = \frac{E_{11}}{1 - \nu_{12}\nu_{21}}; Q_{22} = \frac{E_{22}}{1 - \nu_{12}\nu_{21}}; Q_{12} = \frac{\nu_{21}E_{11}}{1 - \nu_{12}\nu_{21}} \quad (9)$$

$$Q_{66} = G_{12} \quad Q_{55} = G_{13} \quad Q_{44} = G_{23}$$

In this research, the equations of motion or governing equations of CNTRC plate resting on the elastic foundation are obtained by applying the Hamilton's principle and can be written as (Ait Amar Meziane *et al.* 2014, Al-Basyouni *et al.* 2015)

$$\int_t (\partial U_s + \partial U_f + \partial V - \partial K) dt = 0 \quad (10)$$

Where $(\delta U_s, \delta U_f, \delta V$ and $\delta K)$ are the variations of the strain energy, potential energy of elastic foundation, virtual work done by external forces and kinetic energy, respectively. t is time.

The variation of strain energy can be written as

$$\delta U_s = \int_{-h/2}^{h/2} \int_A \left(\sigma_{xx} \delta \epsilon_{xx} + \sigma_{yy} \delta \epsilon_{yy} + \sigma_{xy} \delta \gamma_{xy} + \sigma_{yz} \delta \gamma_{yz} + \sigma_{xz} \delta \gamma_{xz} \right) dA dx \quad (11a)$$

Substituting Eq. (7) into Eq. (11). The Eq. (11) becomes

$$\delta U_s = \int_A \left(N_{xx} \delta u_{0,x} - M_{xx} \delta w_{0,xx} + P_{xx} \delta \rho_{x,x} + N_{yy} \delta v_{0,y} - M_{yy} \delta w_{0,yy} - P_{yy} \delta \rho_{y,y} - N_{xy} (\delta u_{0,y} - \delta v_{0,x}) - 2M_{xy} \delta w_{0,xy} + P_{xy} (\delta \rho_{x,y} + \delta \rho_{y,x}) + R_{yz} \delta \phi_y + R_{xz} \delta \phi_x \right) dx dy \quad (11b)$$

Where, the in-plane forces and moment resultants are defines as

$$(N_{xx}, N_{yy}, N_{xy}) = \int_{-h/2}^{h/2} (\sigma_{xx}, \sigma_{yy}, \sigma_{xy}) dz \quad (12a)$$

$$(M_{xx}, M_{yy}, M_{xy}) = \int_{-h/2}^{h/2} z (\sigma_{xx}, \sigma_{yy}, \sigma_{xy}) dz \quad (12b)$$

$$(P_{xx}, P_{yy}, P_{xy}) = \int_{-h/2}^{h/2} \psi(z) (\sigma_{xx}, \sigma_{yy}, \sigma_{xy}) dz \quad (12c)$$

$$R_{yz} = \int_{-h/2}^{h/2} \frac{\partial \psi(z)}{\partial z} \sigma_{yz} dz, R_{xz} = \int_{-h/2}^{h/2} \frac{\partial \psi(z)}{\partial z} \sigma_{xz} dz \quad (12d)$$

Substituting the Eq. (8) into Eq. (12), the resultants stresses becomes

$$\begin{aligned} \begin{Bmatrix} N_{xx} \\ N_{yy} \\ N_{xy} \end{Bmatrix} &= \begin{bmatrix} A_{11} & A_{12} & 0 \\ A_{12} & A_{22} & 0 \\ 0 & 0 & A_{66} \end{bmatrix} \begin{Bmatrix} \epsilon_{xx}^{(0)} \\ \epsilon_{yy}^{(0)} \\ \epsilon_{xy}^{(0)} \end{Bmatrix} + \begin{bmatrix} B_{11} & B_{12} & 0 \\ B_{12} & B_{22} & 0 \\ 0 & 0 & B_{66} \end{bmatrix} \begin{Bmatrix} \epsilon_{xx}^{(1)} \\ \epsilon_{yy}^{(1)} \\ \epsilon_{xy}^{(1)} \end{Bmatrix} \\ &+ \begin{bmatrix} C_{11} & C_{12} & 0 \\ C_{12} & C_{22} & 0 \\ 0 & 0 & C_{66} \end{bmatrix} \begin{Bmatrix} \epsilon_{xx}^{(\psi)} \\ \epsilon_{yy}^{(\psi)} \\ \epsilon_{xy}^{(\psi)} \end{Bmatrix} \end{aligned} \quad (13a)$$

$$\begin{aligned} \begin{Bmatrix} M_{xx} \\ M_{yy} \\ M_{xy} \end{Bmatrix} &= \begin{bmatrix} B_{11} & B_{12} & 0 \\ B_{12} & B_{22} & 0 \\ 0 & 0 & B_{66} \end{bmatrix} \begin{Bmatrix} \epsilon_{xx}^{(0)} \\ \epsilon_{yy}^{(0)} \\ \epsilon_{xy}^{(0)} \end{Bmatrix} + \begin{bmatrix} D_{11} & D_{12} & 0 \\ D_{12} & D_{22} & 0 \\ 0 & 0 & D_{66} \end{bmatrix} \begin{Bmatrix} \epsilon_{xx}^{(1)} \\ \epsilon_{yy}^{(1)} \\ \epsilon_{xy}^{(1)} \end{Bmatrix} \\ &+ \begin{bmatrix} E_{11} & E_{12} & 0 \\ E_{12} & E_{22} & 0 \\ 0 & 0 & E_{66} \end{bmatrix} \begin{Bmatrix} \epsilon_{xx}^{(\psi)} \\ \epsilon_{yy}^{(\psi)} \\ \epsilon_{xy}^{(\psi)} \end{Bmatrix} \end{aligned} \quad (13b)$$

$$\begin{aligned} \begin{Bmatrix} P_{xx} \\ P_{yy} \\ P_{xy} \end{Bmatrix} &= \begin{bmatrix} C_{11} & C_{12} & 0 \\ C_{12} & C_{22} & 0 \\ 0 & 0 & C_{66} \end{bmatrix} \begin{Bmatrix} \epsilon_{xx}^{(0)} \\ \epsilon_{yy}^{(0)} \\ \epsilon_{xy}^{(0)} \end{Bmatrix} + \begin{bmatrix} E_{11} & E_{12} & 0 \\ E_{12} & E_{22} & 0 \\ 0 & 0 & E_{66} \end{bmatrix} \begin{Bmatrix} \epsilon_{xx}^{(1)} \\ \epsilon_{yy}^{(1)} \\ \epsilon_{xy}^{(1)} \end{Bmatrix} \\ &+ \begin{bmatrix} F_{11} & F_{12} & 0 \\ F_{12} & F_{22} & 0 \\ 0 & 0 & F_{66} \end{bmatrix} \begin{Bmatrix} \epsilon_{xx}^{(\psi)} \\ \epsilon_{yy}^{(\psi)} \\ \epsilon_{xy}^{(\psi)} \end{Bmatrix} \end{aligned} \quad (13c)$$

$$\begin{Bmatrix} R_{yz} \\ R_{xz} \end{Bmatrix} = \begin{bmatrix} H_{44} & 0 \\ 0 & H_{55} \end{bmatrix} \begin{Bmatrix} \gamma_{yz}^{(0)} \\ \gamma_{xz}^{(0)} \end{Bmatrix}, \quad (12d)$$

Where

$$\begin{aligned} \begin{Bmatrix} \epsilon_{xx}^{(0)} \\ \epsilon_{yy}^{(0)} \\ \epsilon_{xy}^{(0)} \end{Bmatrix} &= \begin{Bmatrix} \frac{\partial u_0}{\partial x} \\ \frac{\partial v_0}{\partial y} \\ \frac{\partial u_0}{\partial y} + \frac{\partial v_0}{\partial x} \end{Bmatrix}, \begin{Bmatrix} \epsilon_{xx}^{(1)} \\ \epsilon_{yy}^{(1)} \\ \epsilon_{xy}^{(1)} \end{Bmatrix} = \begin{Bmatrix} -\frac{\partial^2 w_0}{\partial x^2} \\ -\frac{\partial^2 w_0}{\partial y^2} \\ -2\frac{\partial^2 w_0}{\partial x \partial y} \end{Bmatrix}, \\ \begin{Bmatrix} \epsilon_{xx}^{(\psi)} \\ \epsilon_{yy}^{(\psi)} \\ \epsilon_{xy}^{(\psi)} \end{Bmatrix} &= \begin{Bmatrix} \frac{\partial \phi_x}{\partial x} \\ \frac{\partial \phi_y}{\partial y} \\ \frac{\partial \phi_x}{\partial y} + \frac{\partial \phi_y}{\partial x} \end{Bmatrix}, \begin{Bmatrix} \gamma_{yz}^{(0)} \\ \gamma_{xz}^{(0)} \end{Bmatrix} = \begin{Bmatrix} \phi_y \\ \phi_x \end{Bmatrix} \end{aligned} \quad (14)$$

The terms $(A_{ij}, B_{ij}, D_{ij}, C_{ij}, E_{ij}, F_{ij}, H_{ij})$ are the material stiffness components which can be obtained from the followings equations

$$(C_{ij}, E_{ij}, F_{ij}) = \int_{-h/2}^{h/2} \psi(z) Q_{ij} [1, z, \psi(z)] dz \quad i, j = 1, 2, 6 \quad (15a)$$

$$H_{44} = \int_{-h/2}^{h/2} \left(\frac{\partial \psi(z)}{\partial z} \right)^2 Q_{44} dz, H_{55} = \int_{-h/2}^{h/2} \left(\frac{\partial \psi(z)}{\partial z} \right)^2 Q_{55} dz \quad (15b)$$

The first variation of the additional strain energy induced by the elastic foundation can be expressed as

$$\delta U_f = \int_A K_w w_0 \delta w_0 + K_s \left(\frac{\partial w_0}{\partial x} \frac{\partial \delta w_0}{\partial x} + \frac{\partial w_0}{\partial y} \frac{\partial \delta w_0}{\partial y} \right) dx dy, \quad (16)$$

With

$$K_w = \frac{k_w D_0}{a^2}; \quad K_s = \frac{k_g D_0}{a^2}; \quad D_0 = \frac{E^0 h^3}{12(1 - \nu_p^2)} \quad (17)$$

Where k_w is the Winkler constant, k_s is the shear layer spring constant and (β_w, β_s) are the corresponding spring factors which are the given parameters.

The variation of the virtual work done by these external bending loading q can be expressed in the form

$$\delta V = - \int_A q \delta w_0 dx dy \quad (18)$$

The variation of the virtual kinetic energy of the plate can be written as

$$\delta K = \int_A (\dot{u} \delta \dot{u} + \dot{v} \delta \dot{v} + \dot{w} \delta \dot{w}) dx dy dz \quad (19)$$

$$\begin{aligned} \delta K &= \int_A \left\{ I_0 (\dot{u} \delta \dot{u} + \dot{v} \delta \dot{v} + \dot{w} \delta \dot{w}) \right. \\ &+ I_1 \left(\frac{\partial \dot{w}_0}{\partial x} \delta \dot{u}_0 + \frac{\partial \dot{w}_0}{\partial y} \delta \dot{v}_0 + \dot{u}_0 \frac{\partial \delta \dot{w}_0}{\partial x} + \dot{v}_0 \frac{\partial \delta \dot{w}_0}{\partial y} \right) \\ &+ I_2 \left(\frac{\partial \dot{w}_0}{\partial x} \frac{\partial \delta \dot{w}_0}{\partial x} + \frac{\partial \dot{w}_0}{\partial y} \frac{\partial \delta \dot{w}_0}{\partial y} \right) \\ &+ I_3 (\dot{\phi}_x \delta \dot{u}_0 + \dot{u}_0 \delta \dot{\phi}_x + \dot{\phi}_y \delta \dot{v}_0 + \dot{v}_0 \delta \dot{\phi}_y) \\ &+ I_4 \left(\dot{\phi}_x \frac{\partial \delta \dot{w}_0}{\partial x} + \frac{\partial \dot{w}_0}{\partial x} \delta \dot{\phi}_x + \dot{\phi}_y \frac{\partial \delta \dot{w}_0}{\partial y} + \frac{\partial \dot{w}_0}{\partial y} \delta \dot{\phi}_y \right) \\ &\left. + I_5 (\dot{\phi}_x \delta \dot{\phi}_x + \dot{\phi}_y \delta \dot{\phi}_y) \right\} dx dy \end{aligned} \quad (20a)$$

With

$$(I_0, I_1, I_2, I_3, I_4, I_5) = \int_{-h/2}^{h/2} (1, z, z^2, \psi(z), z\psi(z), \psi^2(z)) \rho(z) dz \quad (20b)$$

Where $(I_0, I_1, I_2, I_3, I_4, I_5)$ are mass inertias and $\rho(z)$ is the mass density given in Eq. (2).

Based on the hyperbolic shear deformation theory of CNTRC plate resting on elastic foundation, the equation of motion can be obtained by substituting the variations of the strain energy (δU_s), potential energy of elastic foundation (δU_f), kinetic energy (δK) and the work done by external forces (δV) of Eqs. (11), (16), (18) and (19) into Eq. (10) and after integration by part and collecting the coefficients of $(\delta u_0, \delta v_0, \delta w_0, \delta \phi_x \text{ and } \delta \phi_y)$, the equations of motion can be obtained as

$$\delta u_0 = \frac{\partial N_{xx}}{\partial x} + \frac{\partial N_{xy}}{\partial y} = I_0 \ddot{u}_0 - I_1 \frac{\partial \ddot{w}_0}{\partial x} + I_3 \ddot{\phi}_x \quad (21a)$$

$$\delta v_0 = \frac{\partial N_{yy}}{\partial y} + \frac{\partial N_{xy}}{\partial x} = I_0 \ddot{v}_0 - I_1 \frac{\partial \ddot{w}_0}{\partial y} + I_3 \ddot{\phi}_y \quad (21b)$$

$$\begin{aligned} \delta w_0 = & \frac{\partial^2 M_{xx}}{\partial x^2} + \frac{\partial^2 M_{yy}}{\partial y^2} + 2 \frac{\partial^2 M_{xy}}{\partial x \partial y} - K_w w_0 + K_g \left(\frac{\partial^2 w_0}{\partial x^2} + \frac{\partial^2 w_0}{\partial y^2} \right) + q \\ & + I_1 \left(\frac{\partial \ddot{u}_0}{\partial x} + \frac{\partial \ddot{v}_0}{\partial y} \right) - I_2 \left(\frac{\partial^2 \ddot{w}_0}{\partial x^2} + \frac{\partial^2 \ddot{w}_0}{\partial y^2} \right) + I_4 \left(\frac{\partial \ddot{\phi}_x}{\partial x} + \frac{\partial \ddot{\phi}_y}{\partial y} \right) = I_0 \ddot{w}_0 \end{aligned} \quad (21c)$$

$$\delta \phi_x : \frac{\partial P_{xx}}{\partial y} + \frac{\partial P_{xy}}{\partial x} - R_{yz} = I_3 \ddot{u}_0 - I_4 \frac{\partial \ddot{w}_0}{\partial x} + I_5 \ddot{\phi}_x \quad (21d)$$

$$\delta \phi_y : \frac{\partial P_{yy}}{\partial y} + \frac{\partial P_{xy}}{\partial x} - R_{yz} = I_3 \ddot{v}_0 - I_4 \frac{\partial \ddot{w}_0}{\partial y} + I_5 \ddot{\phi}_y \quad (21e)$$

4. Solution method for bending and vibration problems

Consider a simply supported plate in all edges and placed on the Pasternak elastic foundation, the closed form-solution for bending and vibration problems can be obtained by applying the Navier's procedure, and can be written as

$$u_0(x, y, t) = \sum_{M=1}^{\infty} \sum_{N=1}^{\infty} U_{MN} e^{i\omega t} \cos \alpha x \sin \xi y \quad (22a)$$

$$v_0(x, y, t) = \sum_{M=1}^{\infty} \sum_{N=1}^{\infty} V_{MN} e^{i\omega t} \sin \alpha x \cos \xi y \quad (22b)$$

$$w_0(x, y, t) = \sum_{M=1}^{\infty} \sum_{N=1}^{\infty} W_{MN} e^{i\omega t} \sin \alpha x \sin \xi y \quad (22c)$$

$$\varphi_x(x, y, t) = \sum_{M=1}^{\infty} \sum_{N=1}^{\infty} \Theta_{xMN} e^{i\omega t} \cos \alpha x \sin \xi y \quad (22d)$$

$$\varphi_y(x, y, t) = \sum_{M=1}^{\infty} \sum_{N=1}^{\infty} \Theta_{yMN} e^{i\omega t} \sin \alpha x \cos \xi y \quad (22e)$$

With

$$\alpha = \frac{M\pi}{a}; \xi = \frac{N\pi}{b}; i = \sqrt{-1} \quad (22f)$$

Where U_{MN} , V_{MN} , W_{MN} , Θ_{xMN} and Θ_{yMN} are arbitrary parameters and ω is the frequency of the free vibration.

The transverse load (q) can be given as

$$q(x, y) = \sum_{M=1}^{\infty} \sum_{N=1}^{\infty} Q_{MN} \sin \alpha x \sin \xi y \quad (23)$$

Where

$$q(x, y) = \frac{4}{ab} \int_0^a \int_0^b q(x, y) \sin \alpha x \sin \xi y dx dy \quad (24)$$

In this research, two form of load distribution are used (uniform and sinusoidal) and can be expressed by

$$Q_{MN} = \begin{cases} q_0 (M=N=1) \text{ for sinusoidal load } q_0 \\ \frac{16q_0}{MN\pi^2} (M=N=1,3,5,\dots) \text{ for uniform load } q_0 \end{cases} \quad (25)$$

Substituting the Eqs. (13) and (22) into Eq. (21), the closed form-solutions can be presented in the following matrix form

$$\begin{aligned} & \begin{bmatrix} s_{11} & s_{12} & s_{13} & s_{14} & s_{15} \\ s_{21} & s_{22} & s_{23} & s_{24} & s_{25} \\ s_{31} & s_{32} & s_{33} & s_{34} & s_{35} \\ s_{41} & s_{42} & s_{43} & s_{44} & s_{45} \\ s_{51} & s_{52} & s_{53} & s_{54} & s_{55} \end{bmatrix} \\ & - \omega^2 \begin{bmatrix} m_{11} & m_{12} & m_{13} & m_{14} & m_{15} \\ m_{21} & m_{22} & m_{23} & m_{24} & m_{25} \\ m_{31} & m_{32} & m_{33} & m_{34} & m_{35} \\ m_{41} & m_{42} & m_{43} & m_{44} & m_{45} \\ m_{51} & m_{52} & m_{53} & m_{54} & m_{55} \end{bmatrix} \begin{Bmatrix} U_{MN} \\ V_{MN} \\ W_{MN} \\ \Theta_{xMN} \\ \Theta_{yMN} \end{Bmatrix} = \begin{Bmatrix} 0 \\ 0 \\ Q_{MN} \\ 0 \\ 0 \end{Bmatrix} \end{aligned} \quad (26)$$

With

$$\begin{aligned} s_{11} &= -A_{11}\alpha^2 - A_{66}\xi^2; s_{12} = -A_{12}\alpha \xi - A_{66}\alpha \xi; \\ s_{13} &= B_{11}\alpha^3 + B_{12}\alpha \xi^2 + 2B_{66}\alpha \xi^2; \\ s_{21} &= -A_{11}\alpha \xi - A_{66}\alpha \xi; \\ s_{14} &= -C_{11}\alpha^2 - C_{66}\xi^2; s_{15} = -C_{12}\alpha \xi - C_{66}\alpha \xi; \\ s_{22} &= -A_{22}\xi^2 - A_{66}\alpha^2; s_{23} = B_{12}\alpha^2 \xi + B_{22}\xi^3 + 2B_{66}\alpha^2 \xi; \\ s_{24} &= -C_{12}\alpha \xi - C_{66}\alpha \xi; s_{25} = -C_{22}\xi^2 - C_{66}\alpha^2; \\ s_{31} &= B_{11}\alpha^3 + B_{12}\alpha \xi^2 + 2B_{66}\alpha \xi^2; \\ s_{32} &= B_{12}\alpha^2 \xi + B_{22}\xi^3 + 2B_{66}\alpha^2 \xi; \end{aligned} \quad (27)$$

$$\begin{aligned}
s_{33} &= -D_{11}\alpha^4 - 2D_{12}\alpha^2\xi^2 - D_{22}\xi^4 - 4D_{66}\alpha^2\xi^2 - K_w \\
&- K_g(\alpha^2 + \xi^2); \quad s_{34} = E_{11}\alpha^3 + E_{12}\alpha\xi^2 + 2E_{66}\alpha\xi^2; \\
s_{35} &= E_{12}\alpha^2\xi + E_{22}\xi^3 + 2E_{66}\alpha^2\xi; \quad s_{41} = -C_{11}\alpha^2 - C_{66}\xi^2; \\
s_{42} &= -C_{12}\alpha\xi - C_{66}\alpha\xi; \quad s_{43} = E_{11}\alpha^3 + E_{12}\alpha\xi^2 + 2E_{66}\alpha\xi^2; \\
s_{44} &= -F_{11}\alpha^2 - F_{66}\xi^2 - H_{55}; \quad s_{45} = -F_{12}\alpha\xi + F_{66}\alpha\xi; \\
s_{51} &= -C_{12}\alpha\xi - C_{66}\alpha\xi; \\
s_{25} &= -C_{22}\xi^2 - C_{66}\alpha^2; \quad s_{53} = E_{12}\alpha^2\xi + E_{22}\xi^3 + 2E_{66}\alpha\xi^2; \\
s_{32} &= B_{12}\alpha^2\xi + B_{22}\xi^3 + 2E_{66}\alpha^2\xi; \\
s_{54} &= -F_{12}\alpha\xi - F_{66}\alpha\xi; \quad s_{55} = -F_{22}\xi^2 - F_{66}\alpha^2 - H_{44}
\end{aligned}$$

And

$$\begin{aligned}
m_{11} &= -I_0; \quad m_{12} = 0; \quad m_{13} = I_1\alpha; \quad m_{14} = -I_3; \quad m_{15} = 0; \\
m_{21} &= 0; \quad m_{22} = -I_0; \quad m_{23} = I_1\xi; \quad m_{24} = 0; \quad m_{25} = -I_3; \\
m_{31} &= I_1\alpha; \quad m_{32} = I_1\xi; \quad m_{33} = -I_0 - I_2(\alpha^2 + \xi^2); \quad m_{34} = I_4\alpha; \\
m_{35} &= I_4\xi; \\
m_{41} &= -I_3; \quad m_{42} = 0; \quad m_{43} = I_4\alpha; \quad m_{44} = -I_5; \quad m_{45} = 0; \\
m_{51} &= 0; \quad m_{52} = -I_3; \quad m_{53} = I_4\xi; \quad m_{54} = 0; \quad m_{55} = -I_5
\end{aligned} \quad (28)$$

The followings dimensionless forms used the present numerical results are

For bending

$$\bar{w} = \frac{10^3 D_0 w}{a^4 q_0} \left(\frac{a}{2}, \frac{b}{2} \right); \quad \bar{u} = \frac{10^3 D_0 u}{a^4 q_0} \left(0, \frac{a}{2}, \frac{b}{2} \right); \quad \bar{v} = \frac{10^3 D_0 v}{a^4 q_0} \left(\frac{a}{2}, 0, -\frac{h}{2} \right); \quad (29a)$$

$$\bar{\sigma}_{xx} = \frac{h^2 \sigma_{xx}}{a^2 q_0} \left(\frac{a}{2}, \frac{b}{2}, -\frac{h}{2} \right); \quad \bar{\sigma}_{yy} = \frac{h^2 \sigma_{yy}}{a^2 q_0} \left(\frac{a}{2}, \frac{b}{2}, -\frac{h}{2} \right); \quad (29b)$$

$$\bar{\sigma}_{xy} = \frac{h^2 \sigma_{xy}}{a^2 q_0} \left(0, 0, -\frac{h}{2} \right); \quad \bar{\sigma}_{xz} = \frac{h^2 \sigma_{xz}}{a^2 q_0} \left(0, \frac{b}{2}, -\frac{h}{2} \right). \quad (29c)$$

Where

$$D_0 = \frac{E^p h^3}{12 \left(1 - \left(\nu^p \right)^2 \right)}. \quad (30)$$

For the vibration

$$\bar{\omega} = \omega h \sqrt{\rho^p / E^p} \quad (31)$$

5. Results and discussions

In this section, the accuracy of the present hyperbolic shear deformation plate theory is evaluated. Two types of the plate behavior (bending and the free vibration) will be

studied. For this purpose, the polymer is used as the matrix and the armchair (10,10) SWCNTs are chosen for the material used to reinforce the polymeric matrix in the CNTRC plate. According to the study of Zhu *et al.* (2012) and Wattanasakulpong and Chaikittiratana (2015), the materials properties are

$$\begin{cases} \text{Polymer} : \nu^p = 0.34, \rho^p = 1150 \text{ kg/m}^3, E^p = 2.1 \text{ GPa} \\ \text{SWCNT} : \nu_{12}^{cnt} = 0.175, \rho^{cnt} = 1400 \text{ kg/m}^3, E_{12}^{cnt} = 5.6466 \\ \text{TPa}, E_{22}^{cnt} = 7.0800 \text{ TPa}, G_{12}^{cnt} = G_{12}^{cnt} = G_{12}^{cnt} = 1.9445 \text{ TPa} \end{cases}$$

In the following, several examples of bending and the free vibration of the CNTRC plates will be presented. The results of this model are compared with those of Zhu *et al.* (2012) based on the first shear deformation theory (FSDT), Wattanasakulpong and Chaikittiratana (2015) based on the TSDT (third shear deformation theory) and SSDT (sinusoidal shear deformation theory). The Table 1 presents the comparisons of dimensionless deflection (\bar{w}^*) of square CNTRC plate without elastic foundation under transversal uniform loading ($q_0 = -1.0 \cdot 10^5 \text{ N/m}^2$) for two values of the geometry ratio ($a/h = 10, 20$) and the different patterns of carbon nanotube (UD, X, O and V-plate) and carbon nanotube volume fraction ($\nu_{cnt}^* = 0.11, 0.14$ and 0.17). From the Table1, it can be seen that the present results are in good agreement with those obtained with FSDT, TSDT and SSDT. It is remarkable that the smallest values of the dimensionless deflection are given by a X-type CNT distribution and the largest value are given by the O-plate. So it can be said that the X-plate present the largest capacity to resist the uniform bending load (q_0).

The Table 2 shows the dimensionless deflection (\bar{w}) of different types of CNTRC square plates (UD, X, O and V-plate) for ($a/h = 10$) and different volume fraction values of (ν_{cnt}^*). The plates are under uniform and sinusoidal bending load. It can be seen from the results that the dimensionless deflection is in inverse relation with the spring constant factors, this is due to the harder springs make the stiffer system. It can be noted also that the increase in the volume fraction ν_{cnt}^* leads to a reduction in the dimensionless deflection. The smallest dimensionless deflection values are obtained for X-plate type under sinusoidal bending load.

Table 3 present the dimensionless deflection, normal and shear stresses of CNTRC square plates with elastic foundation ($k_w = 100, k_s = 50$) under uniform load for the different values of thickness ratio ($a/h = 10, 20$ and 30) to show exactly the variations of the in-plane deflection and stresses of the plate. It can be noted that the dimensionless deflection decreases with increase of thickness ratio (a/h).

Table 4 shows a comparison of dimensionless frequencies of isotropic and CNTRC square plates without elastic foundation for ($a/h = 5$ and 10) with different mode of the plate (M, N) and volume fraction ν_{cnt}^* equal 0.17 .

Table 1 Comparisons of dimensionless deflections ($w^* = -10^{-2}(w_0/h)$) of square CNTRC plates without elastic foundation

a/h	V_{cbr}^*	Source	UD	X	O	V
10	0.11	Present	0.3704	0.3115	0.5436	0.4438
		TSDT	0.3717	0.3136	0.5410	0.4450
		SSDT	0.3710	0.3123	0.5429	0.4443
		FSDT	0.3739	0.3177	0.5230	0.4466
	0.14	Present	0.3258	0.2802	0.4686	0.3856
		TSDT	0.3272	0.2822	0.4667	0.3869
		SSDT	0.3264	0.2809	0.4683	0.3861
		FSDT	0.3306	0.2844	0.4525	0.3894
	0.17	Present	0.2373	0.2018	0.3470	0.2855
		TSDT	0.2381	0.2027	0.3459	0.2862
		SSDT	0.2376	0.2022	0.3468	0.2858
		FSDT	0.2394	0.2012	0.3378	0.2864
20	0.11	Present	3.627	2.689	6.251	4.881
		TSDT	3.630	2.695	6.239	4.884
		SSDT	3.628	2.691	6.248	4.883
		FSDT	3.628	2.701	6.155	4.879
	0.14	Present	2.989	2.250	5.136	4.013
		TSDT	2.992	2.255	5.125	4.016
		SSDT	2.990	2.252	5.133	4.015
		FSDT	3.001	2.256	5.070	4.025
	0.17	Present	2.348	1.759	4.065	3.178
		TSDT	2.350	1.751	4.059	3.180
		SSDT	2.349	1.750	4.064	3.179
		FSDT	2.348	1.737	4.020	3.174

Table 2 Dimensionless deflections (\bar{w}) of CNTRC square plates with and without elastic foundation under uniform and sinusoidal loads ($a/h = 10$)

k_w	k_s	Source	$V_{cnt}^* = 0.11$				$V_{cnt}^* = 0.14$				$V_{cnt}^* = 0.17$			
			UD	X	O	V	UD	X	O	V	UD	X	O	V
Uniform load														
0	0	Present	0.7330	0.6163	1.0756	0.8782	0.6447	0.5544	0.9277	0.7630	0.4697	0.3993	0.6867	0.5649
		TSDT	0.7356	0.6206	1.0705	0.8806	0.6475	0.5583	0.9235	0.7656	0.4712	0.4012	0.6844	0.5663
		SSDT	0.7340	0.6179	1.0743	0.8792	0.6458	0.5559	0.9267	0.7640	0.4702	0.4001	0.6862	0.5655
100	0	Present	0.6960	0.5896	0.9999	0.8265	0.6156	0.5326	0.8704	0.7233	0.4541	0.3880	0.6551	0.5432
		TSDT	0.6983	0.5935	0.9955	0.8286	0.6182	0.5362	0.8666	0.7257	0.4556	0.3997	0.6530	0.5444
		SSDT	0.6969	0.5910	0.9988	0.8274	0.6167	0.5339	0.8695	0.7243	0.4548	0.3887	0.6546	0.5437
100	50	Present	0.4763	0.4243	0.6007	0.5338	0.4375	0.3941	0.5514	0.4889	0.3492	0.3088	0.4567	0.3994
		TSDT	0.4773	0.4262	0.5991	0.5346	0.4387	0.3960	0.5498	0.4898	0.3500	0.3098	0.4557	0.4000
		SSDT	0.4767	0.4250	0.6003	0.5341	0.4380	0.3948	0.5510	0.4893	0.3495	0.3092	0.4565	0.3997
Sinusoidal load														
0	0	Present	0.4945	0.4198	0.7111	0.5851	0.4375	0.3790	0.6174	0.5114	0.3165	0.2710	0.4540	0.3758
		TSDT	0.4964	0.4227	0.7081	0.5869	0.4396	0.3817	0.6148	0.5133	0.3177	0.2723	0.4526	0.3769
		SSDT	0.4953	0.4208	0.7104	0.5859	0.4383	0.3800	0.6168	0.5121	0.3170	0.2715	0.4537	0.3763
100	0	Present	0.4712	0.4028	0.6639	0.5528	0.4191	0.3651	0.5815	0.4865	0.3068	0.2639	0.4343	0.3622
		TSDT	0.4729	0.4056	0.6612	0.5544	0.4210	0.3677	0.5792	0.4882	0.3079	0.2651	0.4330	0.3632
		SSDT	0.4719	0.4038	0.6633	0.5534	0.4199	0.3661	0.5809	0.4872	0.3072	0.2644	0.4340	0.3626
100	50	Present	0.3216	0.2882	0.4011	0.3577	0.2965	0.2684	0.3694	0.3287	0.2355	0.2093	0.3040	0.2668
		TSDT	0.3224	0.2896	0.4001	0.3583	0.2974	0.2698	0.3685	0.3295	0.2361	0.2101	0.3034	0.2674
		SSDT	0.3219	0.2888	0.4009	0.3579	0.2969	0.2689	0.3692	0.3290	0.2357	0.2097	0.3039	0.2671

Table 3 Dimensionless deflections and stresses of CNTRC square plates with elastic foundation under uniform load
 $(k_w = 100 ; k_s = 50 ; V_{cnt}^* = 0.17)$

a/h	Plate type	Source	\bar{u}	\bar{v}	\bar{w}	$\bar{\sigma}_{xx}$	$\bar{\sigma}_{yy}$	$\bar{\sigma}_{xy}$
10	UD	Present	0.0333	0.0708	0.3492	0.6905	0.0227	0.0292
		SSDT	0.0332	0.0708	0.3495	0.6882	0.0227	0.0291
	X	Present	0.0245	0.0629	0.3088	0.9998	0.0233	0.0310
		SSDT	0.0244	0.0630	0.3092	0.9962	0.0233	0.0309
	O	Present	0.0545	0.0888	0.4567	0.0277	0.0342	0.0330
		SSDT	0.0543	0.0887	0.4565	0.0277	0.0341	0.0328
	V	Present	0.0552	0.0781	0.3994	0.0268	0.0295	0.0303
		SSDT	0.0551	0.0780	0.3997	0.0268	0.0295	0.0302
	UD	Present	0.0161	0.0269	0.2401	0.6945	0.0147	0.0238
		SSDT	0.0161	0.0270	0.2402	0.6938	0.0147	0.0237
20	X	Present	0.0115	0.0219	0.1874	0.9818	0.0122	0.0237
		SSDT	0.0115	0.0219	0.1875	0.9809	0.0122	0.0236
	O	Present	0.0270	0.0380	0.3684	0.0261	0.0278	0.0287
		SSDT	0.0270	0.0380	0.3683	0.0261	0.0278	0.0286
	V	Present	0.0284	0.0314	0.3059	0.0254	0.0223	0.0268
		SSDT	0.0284	0.0314	0.3059	0.0254	0.0223	0.0267
	UD	Present	0.0161	0.0167	0.2165	0.6940	0.0131	0.0223
		SSDT	0.0106	0.0167	0.2166	0.6937	0.0131	0.0223
	X	Present	0.0075	0.0131	0.1608	0.9746	0.0100	0.0218
		SSDT	0.0075	0.0131	0.1608	0.9741	0.0100	0.0217
30	O	Present	0.0179	0.0244	0.3495	0.0258	0.0265	0.0275
		SSDT	0.0179	0.0244	0.3494	0.0258	0.0265	0.0275
	V	Present	0.0190	0.0198	0.2858	0.0251	0.0208	0.0258
		SSDT	0.0190	0.0198	0.2859	0.0251	0.0208	0.0258

It can be seen that the dimensionless frequencies are in inverse relation with geometry ratio (a/h). The present results are in good agreement with those obtained by the third shear deformation theory (TSDT) and sinusoidal shear deformation theory (SSDT). It should be noted from the results that the lowest values of the frequencies are obtained for an isotropic plate, followed by O-plate, V-plate and UD plate. On the other hand the largest values of the dimensionless frequencies are obtained for the X-plate.

Table 5 illustrate the dimensionless frequencies of CNTRC square plate with and without elastic foundation for ($a/h=10$) and different values of spring constant factors (k_w, k_s). From the table, it can be seen that the presents results are almost identical with those obtained with TSDT and SSDT theories and the dimensionless frequencies of CNTRC plate are in direct correlation relationship with spring constant factors. The most important values of the dimensionless frequencies are obtained for the X-plate type. It can be observed also that the increase of the volume fraction V_{cnt}^* leads to an increase in the dimensionless frequencies.

Fig. 2 shows the dimensionless deflection as a function of the dimension ratio (b/a) for different types of the rectangular plates (UD, X, O and V) resting on elastic foundation under uniform loads with ($a/h=10, k_w=100, k_s=50$ and $V_{cnt}^*=0.17$). It can be noted that the dimensionless deflection increases with increasing of dimension ratio and becomes constant beyond the value ($b/a=1$).

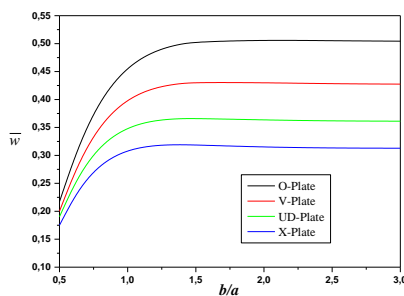
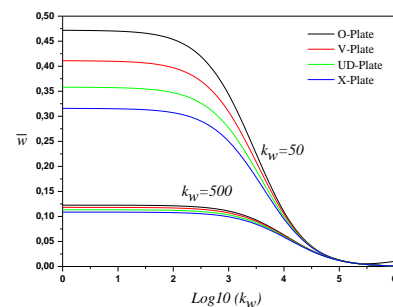
The dimensionless deflection of CNTRC squares plates resting on elastic foundation under uniform load with ($a/h=10, k_w=50, 500$ and $V_{cnt}^*=0.17$) is shown in Fig. 3. The four types of the plates (O, X, V and UD-plate) are studied. It can be noted from the graphs that the dimensionless deflections of CNTRC square plate decreases with increasing of the spring constant factors ($\log_{10}(k_w)$) and the important value of the dimensionless deflection are obtained for O-plate. It can be seen also that the deflection (\bar{w}) tends to zero for the large values of spring constant factors.

Table 4 Comparisons of dimensionless frequencies of isotropic and CNTRC square plates without elastic foundation

a/h	Mode (m,n)	Source	Isotropic	UD	X	O	V
5	(1.1)	Present	0.2133	0.4415	0.4562	0.3990	0.4284
		TSDT	0.2132	0.4383	0.4524	0.3992	0.4258
		SSDT	0.2132	0.4404	0.4549	0.3989	0.4275
		HSDT*	0.2113	-	-	-	-
	(1.2)	Present	0.4649	0.6398	0.6578	0.6122	0.6370
		TSDT	0.4645	0.6372	0.6552	0.6114	0.6347
		SSDT	0.4648	0.6388	0.6569	0.6118	0.6362
		HSDT*	0.4623	-	-	-	-
	(2.2)	Present	0.6713	1.0884	1.1199	0.9995	1.0831
		TSDT	0.6703	1.0650	1.0935	0.9912	1.0610
		SSDT	0.6709	1.0806	1.1115	0.9962	1.0758
		HSDT*	0.6688	-	-	-	-
10	(1.1)	Present	0.0584	0.1687	0.1823	0.1407	0.1546
		TSDT	0.0584	0.1683	0.1819	0.1409	0.1544
		SSDT	0.0584	0.1685	0.1821	0.1408	0.1546
		HSDT*	0.0577	-	-	-	-
	(1.2)	Present	0.1317	0.2203	0.2337	0.1992	0.2124
		TSDT	0.1391	0.2201	0.2334	0.1993	0.2122
		SSDT	0.1392	0.2202	0.2336	0.1992	0.2123
		HSDT*	0.1377	-	-	-	-
	(2.2)	Present	0.2133	0.4415	0.4562	0.3990	0.4284
		TSDT	0.2132	0.4383	0.4524	0.3992	0.4258
		SSDT	0.2132	0.4404	0.4549	0.3989	0.4275
		HSDT*	0.2113	-	-	-	-

Table 5 Dimensionless frequencies of CNTRC square plates with and without elastic foundation ($a/h = 10$)

k_w	k_s	Source	$V_{cnt}^* = 0.11$				$V_{cnt}^* = 0.14$				$V_{cnt}^* = 0.17$			
			UD	X	O	V	UD	X	O	V	UD	X	O	V
0	0	Present	0.1358	0.1474	0.1132	0.1247	0.1439	0.1547	0.1211	0.1330	0.1687	0.1823	0.1407	0.1546
		TSDT	0.1355	0.1469	0.1134	0.1245	0.1436	0.1541	0.1213	0.1328	0.1683	0.1819	0.1409	0.1544
		SSDT	0.1357	0.1472	0.1132	0.1246	0.1438	0.1545	0.1211	0.1329	0.1685	0.1821	0.1408	0.1546
100	0	Present	0.1391	0.1505	0.1171	0.1283	0.1470	0.1576	0.1248	0.1364	0.1713	0.1848	0.1439	0.1575
		TSDT	0.1388	0.1500	0.1173	0.1281	0.1467	0.1570	0.1250	0.1362	0.1710	0.1843	0.1441	0.1573
		SSDT	0.1390	0.1503	0.1172	0.1282	0.1469	0.1574	0.1248	0.1363	0.1712	0.1846	0.1439	0.1574
100	50	Present	0.1684	0.1779	0.1507	0.1595	0.1748	0.1838	0.1565	0.1659	0.1955	0.2074	0.1720	0.1835
		TSDT	0.1682	0.1775	0.1509	0.1594	0.1746	0.1833	0.1567	0.1657	0.1953	0.2070	0.1721	0.1834
		SSDT	0.1683	0.1777	0.1507	0.1595	0.1747	0.1836	0.1566	0.1659	0.1954	0.2073	0.1720	0.1835

Fig. 2 Dimensionless deflections of CNTRC rectangular plates resting on elastic foundation under uniform load ($a/h = 10$; $k_w = 100$; $k_s = 50$; $V_{cnt}^* = 0.17$)Fig. 3 Dimensionless deflections of CNTRC square plates resting on elastic foundation under uniform load ($a/h = 10$; $V_{cnt}^* = 0.17$)

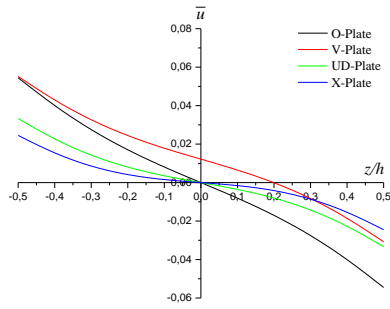


Fig. 4 Dimensionless in-plane deflections of CNTRC square plates with elastic foundation under uniform load ($a/h=10$; $k_w=100, k_g=50, V_{cnt}^*=0.17$)

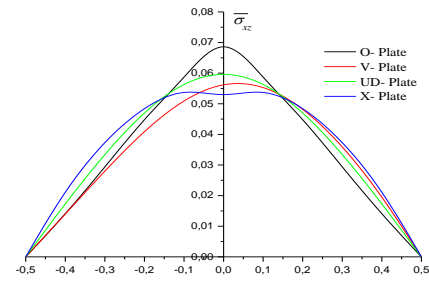
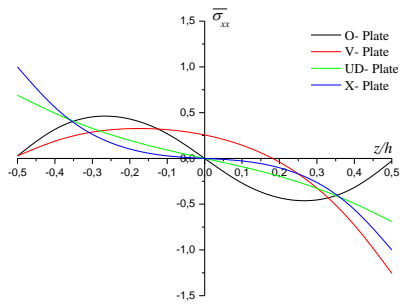


Fig. 5 Dimensionless stresses of CNTRC square plates with elastic foundation under uniform load ($a/h=10$; $k_w=100, k_g=50, V_{cnt}^*=0.17$)

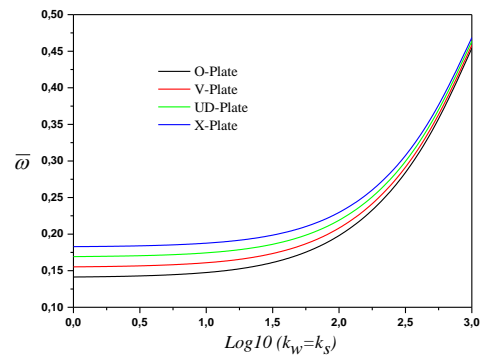
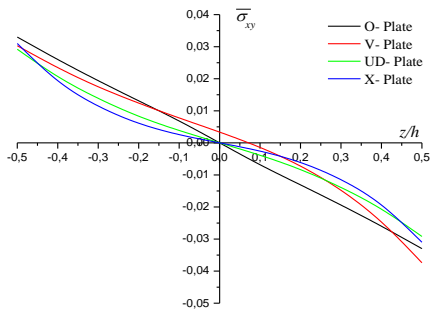
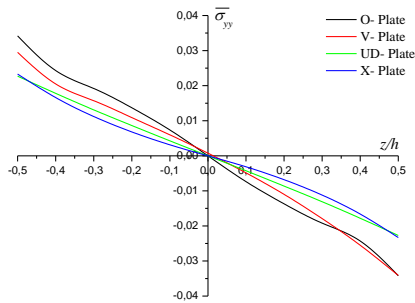


Fig. 6 Dimensionless fundamental frequencies of CNTRC square plates with elastic foundation ($a/h=10$; $V_{cnt}^*=0.17$)



Continued-

The dimensionless In-plane deflection and stresses of CNTRC square plates with elastic foundation ($k_w=100, k_s=50$) as function of the thickness of the plate are illustrate in the Figs. 4 and 5, respectively. It can be observed that from the Fig. 4 that the dimensionless deflections are zero at the mid-plane ($z/h=0$), except that the deflection for V-plate is different to zero ($\bar{w} \neq 0$). It can be seen also from fig. 5 that the dimensionless stresses of V-plate is not zero at mid-plane and the maximum shear stresses is not obtained at the mid-plane, this is due to the unsymmetrical distribution of carbon nanotube (a few amount of carbon nanotube at mid-plane), on the other hand, the maximum of shear stress (σ_{xz}) is obtained at mid-plane and the important values of shear stresses are given by O-plate.

Fig. 6 shows the dimensionless fundamental frequencies ($\bar{w} \neq 0$) of different types of CNTRC squares plates with elastic foundation. It can be seen that the fundamental frequencies increases with increasing of spring constant factors. It can be observed also that for the important values of spring constant factors, the difference between the values of the fundamental frequencies of different plate model (O, X, V and UD) decreases.

6. Conclusions

In this investigation, a new hyperbolic shear deformation theory is developed for study of the bending and the free vibration behaviors of CNTRC plate with and without elastic foundation. Four plates are used in this research such as (O-plate, V-plate, X-plate and UD-plate). Several comparisons have been made to show the accuracy of the present theory. The results are almost identical with those obtained by the existing theories in the literature (FSDT, TSDT and SSDT. It can be concluded that this theory is simple and efficient for the bending and the free vibration of the CNTRC plate and the even on the buckling. An improvement of present formulation will be considered in the future work to consider the thickness stretching effect by using quasi-3D shear deformation models (Bessaim *et al.* 2013, Bousahla *et al.* 2014, Belabed *et al.* 2014, Fekrar *et al.* 2014, Hebali *et al.* 2014, Larbi Chaht *et al.* 2015, Hamidi *et al.* 2015, Bourada *et al.* 2015, Bennoun *et al.* 2016, Draiche *et al.* 2016, Bouafia *et al.* 2017, Benchohra *et al.* 2018, Abualnour *et al.* 2018) and the wave propagation problem (Mahmoud *et al.* 2015, Ait Yahia *et al.* 2015, Boukhari *et al.* 2016, Benadouda *et al.* 2017, Karami *et al.* 2017, Sekkal *et al.* 2017).

Acknowledgments

This research was supported by the Algerian National Thematic Agency of Research in Science and Technology (ATRST) and university of Sidi Bel Abbes (UDL SBA) in Algeria.

References

- Abdelaziz, H.H., Ait Amar Meziane, M., Bousahla, A.A., Tounsi, A., Mahmoud, S.R. and Alwabli, A.S. (2017), "An efficient hyperbolic shear deformation theory for bending, buckling and free vibration of FGM sandwich plates with various boundary conditions", *Steel Compos. Struct.*, **5**(6), 693-704.
- Abualnour, M., Houari, M.S.A., Tounsi, A., Adda Bedia, E.A. and Mahmoud, S.R. (2018), "A novel quasi-3D trigonometric plate theory for free vibration analysis of advanced composite plates", *Compos. Struct.*, **184**, 688-697.
- Ahmed, A. (2014), "Post buckling analysis of sandwich beams with functionally graded faces using a consistent higher order theory", *Int. J. Civil Struct. Environ.*, **4**(2), 59-64.
- Ahouel, M., Houari, M.S.A., Adda Bedia, E.A. and Tounsi, A. (2016) "Size-dependent mechanical behavior of functionally graded trigonometric shear deformable nanobeams including neutral surface position concept", *Steel Compos. Struct.*, **20**(5), 963-981.
- Ait Amar Meziane, M., Abdelaziz, H.H. and Tounsi, A. (2014), "An efficient and simple refined theory for buckling and free vibration of exponentially graded sandwich plates under various boundary conditions", *J. Sandw. Struct. Mater.*, **16**(3), 293-318.
- Ait Yahia, S., Ait Atmane, H., Houari, M.S.A. and Tounsi, A. (2015), "Wave propagation in functionally graded plates with porosities using various higher-order shear deformation plate theories", *Struct. Eng. Mech.*, **53**(6), 1143-1165.
- Ajayan, P.M., Stephen, O., Colliex, C. and Trauth, D. (1994), "Aligned carbon nanotube arrays formed by cutting a polymer resin-nanotube composite", *Science*, **256**, 1212-1214.
- Al-Basyouni, K.S., Tounsi, A. and Mahmoud, S.R. (2015), "Size dependent bending and vibration analysis of functionally graded micro beams based on modified couple stress theory and neutral surface position", *Compos. Struct.*, **125**, 621-630.
- Aldousari, S.M. (2017), "Bending analysis of different material distributions of functionally graded beam", *Appl. Phys. A*, **123**, 296.
- Arani, A.J. and Kolahchi, R. (2016), "Buckling analysis of embedded concrete columns armed with carbon nanotubes", *Comput. Concrete*, **17**(5), 567-578.
- Attia, A., Bousahla, A.A., Tounsi, A., Mahmoud, S.R. and Alwabli, A.S. (2018), "A refined four variable plate theory for thermoelastic analysis of FGM plates resting on variable elastic foundations", *Struct. Eng. Mech.*, (In press).
- Attia, A., Tounsi, A., Adda Bedia, E.A. and Mahmoud, S.R. (2015), "Free vibration analysis of functionally graded plates with temperature-dependent properties using various four variable refined plate theories", *Steel Compos. Struct.*, **18**(1), 187-212.
- Barati, M.R. and Shahverdi, H. (2016), "A four-variable plate theory for thermal vibration of embedded FG nanoplates under non-uniform temperature distributions with different boundary conditions", *Struct. Eng. Mech.*, **60**(4), 707-727.
- Belabed, Z., Houari, M.S.A., Tounsi, A., Mahmoud, S.R. and Anwar Bég, O. (2014), "An efficient and simple higher order shear and normal deformation theory for functionally graded material (FGM) plates", *Compos.: Part B*, **60**, 274-283.
- Beldjelili, Y., Tounsi, A. and Mahmoud, S.R. (2016), "Hygrothermo-mechanical bending of S-FGM plates resting on variable elastic foundations using a four-variable trigonometric plate theory", *Smart Struct. Syst.*, **18**(4), 755-786.
- Belkorissat, I., Houari, M.S.A., Tounsi, A., Adda Bedia, E.A. and Mahmoud, S.R. (2015), "On vibration properties of functionally graded nano-plate using a new nonlocal refined four variable model", *Steel Compos. Struct.*, **18**(4), 1063-1081.
- Bellifa, H., Bakora, A., Tounsi, A., Bousahla, A.A. and Mahmoud, S.R. (2017b), "An efficient and simple four variable refined plate theory for buckling analysis of functionally graded plates", *Steel Compos. Struct.*, **25**(3), 257-270.
- Bellifa, H., Benrahou, K.H., Bousahla, A.A., Tounsi, A. and Mahmoud, S.R. (2017a), "A nonlocal zeroth-order shear deformation theory for nonlinear postbuckling of nanobeams", *Struct. Eng. Mech.*, **62**(6), 695-702.
- Bellifa, H., Benrahou, K.H., Hadji, L., Houari, M.S.A. and Tounsi, A. (2016), "Bending and free vibration analysis of functionally graded plates using a simple shear deformation theory and the concept the neutral surface position", *J. Braz. Soc. Mech. Sci. Eng.*, **38**(1), 265-275.
- Benadouda, M., AitAtmane, H., Tounsi, A., Bernard, F. and Mahmoud, S.R. (2017), "An efficient shear deformation theory for wave propagation in functionally graded material beams with porosities", *Earthq. Struct.*, **13**(3), 255-265.
- Benchohra, M., Driz, H., Bakora, A., Tounsi, A., Adda Bedia, E.A. and Mahmoud, S.R. (2018), "A new quasi-3D sinusoidal shear deformation theory for functionally graded plates", *Struct. Eng. Mech.*, **65**(1), 19-31.
- Bennoun, M., Houari, M.S.A. and Tounsi, A. (2016), "A novel five variable refined plate theory for vibration analysis of functionally graded sandwich plates", *Mech. Adv. Mater. Struct.*, **23**(4), 423-431.
- Bessaim, A., Houari, M.S.A., Tounsi, A., Mahmoud, S.R. and Adda Bedia, E.A. (2013), "A new higher order shear and normal deformation theory for the static and free vibration analysis of sandwich plates with functionally graded isotropic face sheets", *J. Sandw. Struct. Mater.*, **15**, 671-703.
- Bessegghier, A., Houari, M.S.A., Tounsi, A. and Mahmoud, S.R.

- (2017), "Free vibration analysis of embedded nanosize FG plates using a new nonlocal trigonometric shear deformation theory", *Smart Struct. Syst.*, **19**(6), 601 - 614.
- Bilouei, B.S., Kolahchi, R. and Bidgoli, M.R. (2016), "Buckling of concrete columns retrofitted with Nano-Fiber Reinforced Polymer (NFRP)", *Comput. Concrete*, **18**(5), 1053-1063.
- Bouafia, K., Kaci, A., Houari, M.S.A., Benzair, A. and Tounsi, A. (2017), "A nonlocal quasi-3D theory for bending and free flexural vibration behaviors of functionally graded nanobeams", *Smart Struct. Syst.*, **19**(2), 115-126
- Bouderba, B., Houari, M.S.A. and Tounsi, A. (2013), "Thermomechanical bending response of FGM thick plates resting on Winkler-Pasternak elastic foundations", *Steel Compos. Struct.*, **14**(1), 85-104.
- Bouderba, B., Houari, M.S.A. and Tounsi, A. and Mahmoud, S.R. (2016), "Thermal stability of functionally graded sandwich plates using a simple shear deformation theory", *Struct. Eng. Mech.*, **58**(3), 397-422.
- Boukhari, A., Ait Atmane, H., Tounsi, A., Adda Bedia, E.A. and Mahmoud, S.R. (2016), "An efficient shear deformation theory for wave propagation of functionally graded material plates", *Struct. Eng. Mech.*, **57**(5), 837-859.
- Bounouara, F., Benrahou, K.H., Belkorissat, I. and Tounsi, A. (2016), "A nonlocal zeroth-order shear deformation theory for free vibration of functionally graded nanoscale plates resting on elastic foundation", *Steel Compos. Struct.*, **20**(2), 227-249.
- Bourada, M., Kaci, A., Houari, M.S.A. and Tounsi, A. (2015), "A new simple shear and normal deformations theory for functionally graded beams", *Steel Compos. Struct.*, **18**(2), 409-423.
- Bousahla, A.A., Benyoucef, S., Tounsi, A. and Mahmoud, S.R. (2016), "On thermal stability of plates with functionally graded coefficient of thermal expansion", *Struct. Eng. Mech.*, **60**(2), 313-335.
- Bousahla, A.A., Houari, M.S.A., Tounsi, A. and Adda Bedia, E.A. (2014), "A novel higher order shear and normal deformation theory based on neutral surface position for bending analysis of advanced composite plates", *Int. J. Comput. Meth.*, **11**(6), 1350082.
- Chikh, A., Tounsi, A., Hebali, H. and Mahmoud, S.R. (2017), "Thermal buckling analysis of cross-ply laminated plates using a simplified HSDT", *Smart Struct. Syst.*, **19**(3), 289-297.
- Draiche, K., Tounsi, A. and Mahmoud, S.R. (2016), "A refined theory with stretching effect for the flexure analysis of laminated composite plates", *Geomech. Eng.*, **11**(5), 671-690.
- Ebrahimi, F. and Habibi, S. (2016), "Deflection and vibration analysis of higher-order shear deformable compositionally graded porous plate", *Steel Compos. Struct.*, **20**(1), 205-225.
- El-Haina, F., Bakora, A., Bousahla, A.A., Tounsi, A. and Mahmoud, S.R. (2017), "A simple analytical approach for thermal buckling of thick functionally graded sandwich plates", *Struct. Eng. Mech.*, **63**(5), 585-595.
- Esawi, A.M. and Farag, M.M. (2007), "Carbon nanotube reinforced composites: potential and current challenges", *Mater. Des.*, **28**(9), 2394-2401.
- Fadelus, J.D., Wiesel, E., Gojny, F.H., Schulte, K. and Wagner, H.D. (2005), "Thermo-mechanical properties of randomly oriented carbon/epoxy nanocomposites", *Compos. Part A*, **36**, 1555-1561.
- Fahsi, A., Tounsi, A., Hebali, H., Chikh, A., Adda Bedia, E.A. and Mahmoud, S.R. (2017), "A four variable refined nth-order shear deformation theory for mechanical and thermal buckling analysis of functionally graded plates", *Geomech. Eng.*, **13**(3), 385-410.
- Fekrar, A., Houari, M.S.A., Tounsi, A. and Mahmoud, S.R. (2014), "A new five-unknown refined theory based on neutral surface position for bending analysis of exponential graded plates", *Meccanica*, **49**, 795-810.
- Ghorbanpour Arani, A., Cheraghbak, A. and Kolahchi, R. (2016), "Dynamic buckling of FGM viscoelastic nano-plates resting on orthotropic elastic medium based on sinusoidal shear deformation theory", *Struct. Eng. Mech.*, **60**(3), 489-505.
- Griebel, M. and Hamaekers, J. (2004), "Molecular dynamics simulations of the elastic moduli of polymer carbon nanotube composites", *Comput. Method. Appl. M.*, **193**, 1773-1788.
- Hachemi, H., Kaci, A., Houari, M.S.A., Bourada, A., Tounsi, A. and Mahmoud, S.R. (2017), "A new simple three-unknown shear deformation theory for bending analysis of FG plates resting on elastic foundations", *Steel Compos. Struct.*, **25**(6), 717-726.
- Hajmohammad, M.H., Zarei, M.S., Nouri, A. and Kolahchi, R. (2017), "Dynamic buckling of sensor/functionally graded-carbon nanotube-reinforced laminated plates/actuator based on sinusoidal-visco-piezoelectricity theories", *J. Sandw. Struct. Mater.*, (In press).
- Hamidi, A., Houari, M.S.A., Mahmoud, S.R. and Tounsi, A. (2015), "A sinusoidal plate theory with 5-unknowns and stretching effect for thermomechanical bending of functionally graded sandwich plates", *Steel Compos. Struct.*, **18**(1), 235-253.
- Han, Y. and Elliott, J. (2007), "Molecular dynamics simulations of the elastic properties of polymer/carbon nanotube composites", *Comput. Mater. Sci.*, **39**, 315-323.
- Hebali, H., Tounsi, A., Houari, M.S.A., Bessaim, A. and Adda Bedia, E.A. (2014), "A new quasi-3D hyperbolic shear deformation theory for the static and free vibration analysis of functionally graded plates", *J. Eng. Mech.-ASCE*, **140**, 374-383.
- Houari, M.S.A., Tounsi, A., Bessaim, A. and Mahmoud, S.R. (2016), "A new simple three unknown sinusoidal shear deformation theory for functionally graded plates", *Steel Compos. Struct.*, **22**(2), 257 - 276.
- Hu, N., Fukunaga, H., Lu, C., Kameyama, M. and Yan, B. (2005), "Prediction of elastic properties of carbon nanotube reinforced composites", *Proc. R. Soc. A*, **461**, 1685-1710.
- Karami, B., Janghorban, M. and Tounsi, A. (2017), "Effects of triaxial magnetic field on the anisotropic nanoplates", *Steel Compos. Struct.*, **25**(3), 361-374.
- Khetir, H., Bachir Bouiadja, M., Houari, M.S.A., Tounsi, A., S.R. Mahmoud, (2017), "A new nonlocal trigonometric shear deformation theory for thermal buckling analysis of embedded nanosize FG plates", *Struct. Eng. Mech.*, **64**(4), 391-402.
- Klouche, F., Darcherif, L., Sekkal, M., Tounsi, A. and Mahmoud, S.R. (2017), "An original single variable shear deformation theory for buckling analysis of thick isotropic plates", *Struct. Eng. Mech.*, **63**(4), 439-446.
- Kolahchi, R. (2017), "A comparative study on the bending, vibration and buckling of viscoelastic sandwich nano-plates based on different nonlocal theories using DC, HDQ and DQ methods", *Aerosp. Sci. Technol.*, **66**, 235-248.
- Kolahchi, R. and Bidgoli, A.M. (2016), "Size-dependent sinusoidal beam model for dynamic instability of single-walled carbon nanotubes", *Appl. Math. Mech.*, **37**(2), 265-274.
- Kolahchi, R. and Cheraghbak, A. (2017), "Agglomeration effects on the dynamic buckling of viscoelastic microplates reinforced with SWCNTs using Bolotin method", *Nonlinear Dynam.*, **90**(1), 479-492.
- Kolahchi, R., Hosseini, H. and Esmailpour, M. (2016a), "Differential cubature and quadrature-Bolotin methods for dynamic stability of embedded piezoelectric nanoplates based on visco-nonlocal-piezoelectricity theories", *Compos. Struct.*, **157**, 174-186.
- Kolahchi, R., Keshtegar, B. and Fakhar, M.H. (2017b), "Optimization of dynamic buckling for sandwich nanocomposite plates with sensor and actuator layer based on sinusoidal-visco-piezoelectricity theories using Grey Wolf

- algorithm", *J. Sandw. Struct. Mater.*, (In press).
- Kolahchi, R., Zarei, M.S., Hajmohammad, M.H. and Nouri, A. (2017b), "Wave propagation of embedded viscoelastic FG-CNT-reinforced sandwich plates integrated with sensor and actuator based on refined zigzag theory", *Int. J. Mech. Sci.*, **130**, 534-545.
- Kolahchi, R., Zarei, M.S., Hajmohammad, M.H. and Nouri, A. (2017c), "Wave propagation of embedded viscoelastic FG-CNT-reinforced sandwich plates integrated with sensor and actuator based on refined zigzag theory", *Int. J. Mech. Sci.*, **130**, 534-545.
- Kolahchi, R., Zarei, M.S., Hajmohammad, M.H. and Oskouei, A.N. (2017a), "Visco-nonlocal-refined Zigzag theories for dynamic buckling of laminated nanoplates using differential cubature-Bolotin methods", *Thin-Walled Struct.*, **113**, 162-169.
- Kolahchi, R., Safari, M., Esmailpour, M. (2016b), "Dynamic stability analysis of temperature-dependent functionally graded CNT-reinforced visco-plates resting on orthotropic elastomeric medium", *Composite Structures*, **150**, 255-265.
- Larbi Chaht, F., Kaci, A., Houari, M.S.A., Tounsi, A., Anwar Bég, O. and Mahmoud, S.R. (2015), "Bending and buckling analyses of functionally graded material (FGM) size-dependent nanoscale beams including the thickness stretching effect", *Steel Compos. Struct.*, **18**(2), 425-442.
- Lau, A.K.T. and Hui, D. (2002), "The revolutionary creation of new advanced materials—carbon nanotube composites", *Compos. Part B: Engineering*, **33**(4), 263-277.
- Lau, K.T. et al. (2004), "Stretching process of single-and multi-walled carbon nanotubes for nanocomposite applications", *Carbon*, **42**(2), 426-428.
- Lei, Z.X., Liew, K.M. and Yu, J.L. (2013), "Buckling analysis of functionally graded carbon nanotube-reinforced composite plates using the element-free kp-Ritz method", *Compos. Struct.*, **98**, 160-168.
- Madani, H., Hosseini, H. and Shokravi, M. (2016), "Differential cubature method for vibration analysis of embedded FG-CNT-reinforced piezoelectric cylindrical shells subjected to uniform and non-uniform temperature distributions", *Steel Compos. Struct.*, **22**(4), 889-913.
- Mahi, A., Adda Bedia, E.A. and Tounsi, A. (2015), "A new hyperbolic shear deformation theory for bending and free vibration analysis of isotropic, functionally graded, sandwich and laminated composite plates", *Appl. Math. Model.*, **39**(9), 2489-2508.
- Mahmoud, S.R., Abd-Alla, A.M., Tounsi, A. and Marin, M. (2015), "The problem of wave propagation in magneto-rotating orthotropic non-homogeneous medium", *J. Vib. Control*, **21**(16), 3281-3291.
- Mehar, K. and Panda, S. (2017b), "Thermoelastic nonlinear frequency analysis of CNT reinforced functionally graded sandwich structure", *Eur. J. Mech. - A/Solids*, **65**, 384-396.
- Mehar, K. and Panda, S.K. (2017a), "Thermoelastic analysis of FG-CNT reinforced shear deformable composite plate under various loading", *Int. J. Comput. Meth.*, **14**(2), 1750019.
- Meksi, R., Benyoucef, S., Mahmoudi, A., Tounsi, A., Adda Bedia, E.A. and Mahmoud, S.R. (2018), "An analytical solution for bending, buckling and vibration responses of FGM sandwich plates", *J. Sandw. Struct. Mater.*, 1099636217698443.
- Menasria, A., Bouhadra, A., Tounsi, A., Bousahla, A.A. and Mahmoud, S.R. (2017), "A new and simple HSDT for thermal stability analysis of FG sandwich plates", *Steel Compos. Struct.*, **25**(2), 157-175.
- Mokashi, V.V., Qian, D. and Liu, Y.J. (2007), "A study on the tensile response and fracture in carbon nanotube-based composites using molecular mechanics", *Compos. Sci. Technol.*, **67**, 530-540.
- Mouffoki, A., AddaBedia, E.A., Houari, M.S.A., Tounsi, A. and Mahmoud, S.R. (2017), "Vibration analysis of nonlocal advanced nanobeams in hygro-thermal environment using a new two-unknown trigonometric shear deformation beam theory", *Smart Struct. Syst.*, **20**(3), 369-383.
- Odegard, G.M., Gates, T.S., Wise, K.E., Park, C. and Siochi, E.J. (2003), "Constitutive modelling of nanotube-reinforced polymer composites", *Compos. Sci. Technol.*, **63**, 1671-1687.
- Sekkal, M., Fahsi, B., Tounsi, A. and Mahmoud, S.R. (2017a), "A novel and simple higher order shear deformation theory for stability and vibration of functionally graded sandwich plate", *Steel Compos. Struct.*, **25**(4), 389-401.
- Sekkal, M., Fahsi, B., Tounsi, A. and Mahmoud, S.R. (2017b), "A new quasi-3D HSDT for buckling and vibration of FG plate", *Struct. Eng. Mech.*, **64**(6), 737-749.
- Shen, H.S. (2009), "Nonlinear bending of functionally graded carbon nanotube-reinforced composite plates in thermal environments", *Compos. Struct.*, **91**, 9-19.
- Shen, H.S. and Zhang, C.L. (2010), "Thermal buckling and postbuckling behavior of functionally graded carbon nanotube-reinforced composite plates", *Mater. Des.*, **31**, 3403-3411.
- Shokravi, M. (2017a), "Dynamic pull-in and pull-out analysis of viscoelastic nanoplates under electrostatic and Casimir forces via sinusoidal shear deformation theory", *Microelectron. Reliab.*, **71**, 17-28.
- Shokravi, M. (2017b), "Vibration analysis of silica nanoparticles-reinforced concrete beams considering agglomeration effects", *Comput. Concrete*, **19**(3), 333-338.
- Shokravi, M. (2017c), "Buckling analysis of embedded laminated plates with agglomerated CNT-reinforced composite layers using FSDT and DQM", *Geomech. Eng.*, **12**(2), 327-346.
- Shokravi, M. (2017d), "Buckling of sandwich plates with FG-CNT-reinforced layers resting on orthotropic elastic medium using Reddy plate theory", *Steel Compos. Struct.*, **23**(6), 623-631.
- Taibi, F.Z., Benyoucef, S., Tounsi, A., Bachir Bouiadjra, R., Adda Bedia, E.A. and Mahmoud, S.R. (2015), "A simple shear deformation theory for thermo-mechanical behaviour of functionally graded sandwich plates on elastic foundations", *J. Sandw. Struct. Mater.*, **17**(2), 99 - 129.
- Thai, H.T. and Kim, S.E. (2013), "A simple higher-order shear deformation theory for bending and free vibration analysis of functionally graded plates", *Compos. Struct.*, **96**, 165-173.
- Tounsi, A., Houari, M.S.A., Benyoucef, S. and Adda Bedia, E.A. (2013), "A refined trigonometric shear deformation theory for thermoelastic bending of functionally graded sandwich plates", *Aerosp. Sci. Technol.*, **24**(1), 209-220.
- Wang, Z.X. and Shen, H.S. (2011), "Nonlinear vibration of nanotube-reinforced composite plates in thermal environments", *Comput. Mater. Sci.*, **50**, 2319-2330.
- Wattanasakulpong, N. and Chaikittiratanana, A. (2015), "Exact solutions for static and dynamic analyses of carbon nanotube-reinforced composite plates with Pasternak elastic foundation", *Appl. Math. Model.*, **39**(18), 5459-5472.
- Xie, X.L., Mai, Y.W. and Zhou, X.P. (2005), "Dispersion and alignment of carbon nanotubes in polymer matrix: a review", *Mater. Sci. Eng.*, **49**, 89-112.
- Yazid, M., Heireche, H., Tounsi, A., Bousahla, A.A. and Houari, M.S.A. (2018), "A novel nonlocal refined plate theory for stability response of orthotropic single-layer graphene sheet resting on elastic medium", *Smart Struct. Syst.*, **21**(1), 15-25.
- Youcef, D.O., Kaci, A., Benzair, A., Bousahla, A.A. and Tounsi, A. (2018), "Dynamic analysis of nanoscale beams including surface stress effects", *Smart Struct. Syst.*, **21**(1), 65-74.
- Zamanian, M., Kolahchi, R. and Bidgoli, M.R. (2017), "Agglomeration effects on the buckling behaviour of embedded concrete columns reinforced with SiO₂ nano-particles", *Wind Struct.*, **24**(1), 43-57.
- Zarei, M.S., Kolahchi, R., Hajmohammad, M.H. and Maleki, M. (2017), "Seismic response of underwater fluid-conveying

- concrete pipes reinforced with SiO₂ nanoparticles and fiber reinforced polymer (FRP) layer”, *Soil Dyn. Earthq. Eng.*, **103**, 76-85.
- Zemri, A., Houari, M.S.A., Bousahla, A.A. and Tounsi, A. (2015), “A mechanical response of functionally graded nanoscale beam: an assessment of a refined nonlocal shear deformation theory beam theory”, *Struct. Eng. Mech.*, **54**(4), 693-710
- Zhu, P., Lei, Z.X. and Liew, K.M. (2012), “Static and free vibration analyses of carbon nanotube-reinforced composite plates using finite element method with first order shear deformation plate theory”, *Compos Struct.*, **94**, 1450-1460.
- Zhu, R., Pan, E. and Roy, A.K. (2007), “Molecular dynamics study of the stress-strain behavior of carbon-nanotube reinforced Epon 862 composites”, *Mater. Sci. Eng. A*, **447**, 51-57.
- Zidi, M., Houari, M.S.A., Tounsi, A., Bessaim, A. and Mahmoud, S.R. (2017), “A novel simple two-unknown hyperbolic shear deformation theory for functionally graded beams”, *Struct. Eng. Mech.*, **64**(2), 145-153.
- Zidi, M., Tounsi, A., Houari M.S.A., AddaBedia, E.A. and Anwar Bég, O. (2014), “Bending analysis of FGM plates under hygro thermo-mechanical loading using a four variable refined plate theory”, *Aerosp. Sci. Technol.*, **34**, 24-34.
- Zine, A., Tounsi, A., Draiche, K., Sekkal, M. and Mahmoud, S.R. (2018), “A novel higher-order shear deformation theory for bending and free vibration analysis of isotropic and multilayered plates and shells”, *Steel Compos. Struct.*, **26**(2), 125-137.